

KINETICS AND THERMOCHEMISTRY OF THE OXIDATION OF UNSATURATED RADICALS: $n\text{-C}_4\text{H}_5 + \text{O}_2$

D. Gutman, I. R. Slagle, A. Bencsura, and S.-B. Xing
Department of Chemistry
Catholic University of America
Washington, DC 20064

Keywords: unsaturated radicals; $\text{C}_4\text{H}_5 + \text{O}_2$; $\text{C}_4\text{H}_5 + \text{C}_2\text{H}_2$

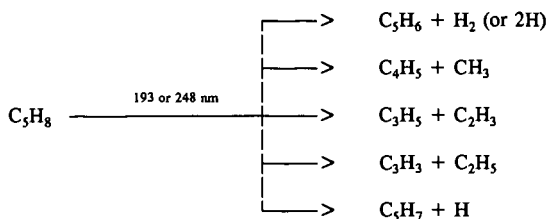
INTRODUCTION

The reactions of unsaturated free radicals (such as C_3H_3 and C_4H_5) either with themselves or with small unsaturated molecules have been proposed as pathways leading to the eventual formation of aromatic compounds and soot.¹ Little is known about the reactions of these intermediates. In particular, the chemistry of the butadienyl radical (C_4H_5) is almost completely unknown. In order to test the feasibility of this radical as a soot precursor, it is important to determine if molecular oxygen can compete as a radical sink for C_4H_5 in combustion systems, preventing the growth of $[\text{C}_4\text{H}_5]$ to levels where reactions producing aromatic compounds can occur at a measurable rate. In this paper we report a direct experimental study of the kinetics and thermochemistry of the reaction of C_4H_5 with O_2 and use the results obtained to infer some general mechanistic pathways for the reactions of hydrogen-deficient free radicals with molecular oxygen.

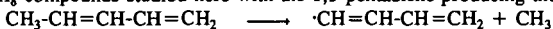
EXPERIMENTAL

Apparatus and General Procedure Details of the experimental apparatus and procedures have been published elsewhere² and only those aspects of the method which are unique to the present study will be described in detail here. Pulsed, unfocused 193-nm or 248-nm radiation (≈ 5 Hz) from a Lambda Physik EMG 201 MSC excimer laser was directed along the axis of a heatable, boric acid-coated quartz reactor (1.05-cm-i.d.). Gas flowing through the tube at ≈ 4 m s^{-1} contained the butadienyl radical precursor (trans-1,3-pentadiene) in small amounts, oxygen, and helium. The flowing gas was completely replaced between laser pulses. Gas was sampled through a hole (0.043-cm diameter) located at the end of a nozzle in the side of the reactor and formed into a beam by a conical skimmer before the gas entered the vacuum chamber containing the photoionization mass spectrometer (PIMS). As the gas beam traversed the ion source, a portion was photoionized using resonance lamps (10.2 and 8.9-9.1 eV) and mass selected. Temporal ion signal profiles of the reactant radical, products and the radical precursor were recorded on a multichannel scalar from a short time before each laser pulse up to 20 ms following the pulse. Data from 1000 to 45,000 repetitions of the experiment were accumulated before the data were analyzed.

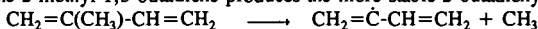
Photolysis of Butadienyl Radical Precursors and the Nature of the C_4H_5 Radical A survey was conducted to determine the products of the photolysis of two possible C_4H_5 radical precursors: trans-1,3-pentadiene (expected to produce the 1-butadienyl radical) and 2-methyl-1,3-butadiene (expected to produce the 2-butadienyl radical). This survey was conducted at two photolysis wavelengths (193 and 248 nm) and two temperatures (298 and 650K). The mass spectrometric results were essentially the same at both wavelengths, with either precursor, and at either temperature. The largest ion signal detected after photolysis corresponded to the mass of C_5H_6 , a stable product. Smaller signals of approximately equal amplitude were detected at the mass numbers corresponding to C_4H_5 , C_3H_5 , C_3H_3 and C_3H_7 . These ion signals exhibited the temporal behavior of free radicals with the signals decaying in an exponential manner due to the presence of heterogeneous wall effects. Smaller amounts of CH_3 , C_2H_3 , C_2H_5 , C_3H_6 , and C_4H_4 were also detected. These results indicate that the important photolysis routes are



While PIMS is a sensitive method for detecting small concentrations of free radicals (even in the presence of large concentrations of radical precursors), it cannot distinguish between structural isomers unless the ionization potentials of these isomers are extremely different. Such is not the case for the C_4H_5 isomers. However, it is likely that the initial photolysis occurs at different sites in the two C_5H_8 compounds studied here with the 1,3-pentadiene producing the 1-butadienyl radical,



while the 2-methyl-1,3-butadiene produces the more stable 2-butadienyl radical.



Although PIMS cannot distinguish between these two structural forms (or between a third form common to both precursors), a difference in observed reactivity can indicate the presence of two distinct isomers. At very low initial concentrations where radical-radical reactions are unimportant and in the absence of any other reactants, both possible C_4H_5 species react in a similar manner, displaying a simple exponential decay due to the presence of heterogeneous effects. However, when molecular oxygen is added to the system, there is a distinct difference in the temporal behavior of the two species. At room temperature in the presence of added oxygen the C_4H_5 produced from the pentadiene reacts slowly and decays in a purely exponential manner. On the other hand, the C_4H_5 from the methylbutadiene reacts much more rapidly with a temporal behavior that is bi-exponential (perhaps indicating the presence of two structural forms of C_4H_5 with very different reactivities). At higher temperatures in the presence of oxygen, the temporal ion signal profiles of both species exhibit bi-exponential behavior but with extremely different time constants, the C_4H_5 from the methylbutadiene always decaying much more rapidly than that from the pentadiene. On the basis of this difference in reactivity we conclude that the C_4H_5 produced from the 1,3-pentadiene is indeed the 1-butadienyl radical.

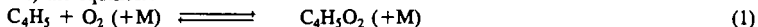
Measurement of $\text{C}_4\text{H}_5 + \text{O}_2$ Reaction Rate Parameters In the experiments reported here the 1-butadienyl radical was produced in presence of varying amounts of oxygen by the 193- or 248-nm photolysis of 1,3-pentadiene. Initial radical concentrations were chosen to be low enough to ensure that radical-radical recombination reactions, either of C_4H_5 with itself or with the other products of the photolysis, had negligible rates compared to the reaction of interest. The absence of radical-radical reactions was confirmed at each set of experimental conditions reported here by varying the initial pentadiene precursor concentration. These tests also confirmed that the reaction of C_4H_5 with C_5H_8 had a negligible rate under these conditions. Reaction rate parameters were also found to be independent of laser wavelength and intensity. These tests ensure that the $1-\text{C}_4\text{H}_5 + \text{O}_2$ reaction was in fact isolated for direct study.

Search for Products of the $\text{C}_4\text{H}_5 + \text{O}_2$ Reaction The search for possible products of the $\text{C}_4\text{H}_5 + \text{O}_2$ reaction was hampered by the production of the additional C_5H_8 photolysis products, the low concentrations of C_4H_5 radicals necessary to avoid recombination reactions, and the high oxygen concentrations used in this study. The photolysis of pentadiene produces many radicals which are themselves possible products of the $\text{C}_4\text{H}_5 + \text{O}_2$ reaction or which react more rapidly with O_2 than C_4H_5 to produce the same possible products. For example, C_3H_4 , a stable photolysis product, is also the product expected from either the direct abstraction of a hydrogen atom from C_4H_5 by O_2 or by the subsequent decomposition of a $\text{C}_4\text{H}_5\text{O}_2$ adduct. Another photolysis product, C_2H_3 , reacts rapidly

with O₂ to produce H₂CO while C₃H₃ + O₂ produces ketene at high temperatures. The C₄H₅O₂ adduct itself could not be detected. This was not unexpected since alkylperoxy radicals are not readily detected by PIMS. Another possible product, C₄H₄O, could not be detected because it lies at the same mass number as the precursor molecule. C₃H₄O, a product analogous to the ketene produced in the high-temperature C₃H₃ + O₂ reaction, was observed at 900K, but could not be confirmed as a product of the C₄H₅ + O₂ reaction since its temporal behavior did not mirror that of the C₄H₅ radical. There were no product signals detected that could be unambiguously assigned to the C₄H₅ + O₂ reaction. Since the mechanism for this reaction could not be established by direct methods, it will be assigned based on rate data and using analogies with what is known about the mechanisms of the reactions of similar unsaturated radicals.

RESULTS

From a preliminary set of experiments conducted over the temperature range of this study (295 - 900K), it was discovered that the 1-C₄H₅ + O₂ reaction has different mechanisms at low and high temperatures and that at intermediate temperatures (369 - 409K at the oxygen pressures used in these experiments) the equilibrium



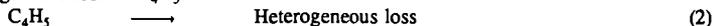
is clearly established.

The results obtained will be discussed separately for the three temperature ranges in which different kinetic behavior was observed. Rate constants were measured at three densities at room temperature and at two densities in the high temperature region. Equilibrium constants for reaction 1 were determined in the intermediate region. The conditions of all these experiments and the results obtained are given in Table I and plotted in Figures 1 and 2.

Room Temperature Reaction Near room temperature the C₄H₅ + O₂ reaction proceeds by simple addition



The temporal behavior of C₄H₅ in the presence of an excess of O₂ can be characterized by a simple first-order decay, with a decay constant (k') equal to the sum of k₁[O₂] and k₂ where k₂ is the rate for the heterogeneous loss of C₄H₅.



The bimolecular rate constant was obtained from the slope of the line fitted through the measured decay constants plotted against [O₂]. From the density dependence of this rate constant ($\Delta \log(k)/\Delta \log[M] \approx 0.4$, it is apparent that the reaction is near the middle of the fall-off region at the densities used in this study ($6-18 \times 10^{16}$ molecule cm⁻³). (See Figure 1.) The addition mechanism is inferred from this density dependence of the rate constant as well as the fact that the reaction is reversible at higher temperatures.

Intermediate Temperature Range Between 369 and 409K the loss of C₄H₅ in the presence of O₂ was not a simple exponential decay but was rather a rapid decay followed by a much slower one which is characteristic of the radical reaching an observable equilibrium with O₂, reaction 1. The second, slower decay is due to competing processes, such as the heterogeneous removal of C₄H₅ at the walls (reaction 2), other possible reactions of C₄H₅ with O₂, or other reactions of C₄H₅O₂ that produce products other than the original reactants. As can be seen in Table Ib, this second decay constant, m₂, increases with temperature while the wall loss rate (reaction 2) remains essentially constant. This observation indicates that a change in reaction mechanism is occurring in this temperature range. This conclusion is supported by the fact that an observable reaction of C₄H₅ with O₂ continues to occur at higher temperatures (see below), where normally equilibrium of C₄H₅ and C₄H₅O₂ would be established before measurable amounts of C₄H₅ had reacted with O₂.

The equilibrium constant, K₁, was obtained from the parameters of the double exponential function³ which was fit to the experimental C₄H₅ ion signal profiles in this temperature range. The relationship between K₁ and these parameters is determined by the mechanism responsible for the temporal behavior of the C₄H₅. From the presence of a high temperature reaction and by analogy with reactions of other radicals, such as ethyl and propargyl, which exhibit similar behavior, we

conclude that the $C_4H_5 + O_2$ mechanism involves three steps: reversible addition (reaction 1), heterogeneous loss of C_4H_5 (reaction 2) and the unimolecular decomposition of the $C_4H_5O_2$ adduct.



Thermodynamic functions for reaction 1 were obtained from the temperature dependence of K_1^2 . The values of ΔH_{298}° and ΔS_{298}° were determined from the slope and the intercept of the straight line fitted through the measured equilibrium constants on a modified van't Hoff plot (see Figure 2). They are

$$\begin{aligned} \Delta H_{298}^\circ &= -18.7 \pm 0.8 \text{ kcal mol}^{-1} \\ \Delta S_{298}^\circ &= -29.8 \pm 2.2 \text{ cal mol}^{-1} \text{ K}^{-1} \end{aligned}$$

The correction to the ordinate variable, $\ln K_p$, on the modified van't Hoff plot (which converts $-\Delta G^\circ_T/RT$ to $-\Delta G^\circ_{298}/RT$) is small (0.7 to 2%) and is obtained from heat capacities estimated by using group-additivity rules.

High Temperature Reaction (600 - 900K) Above the temperature at which equilibrium can be observed, C_4H_5 continues to react with O_2 . Radical decay profiles in this temperature region are again simple exponential functions and the decay constants (k') are proportional to $[O_2]$. The phenomenological bimolecular rate constants are independent of a factor of two in density ($6 - 12 \times 10^{16}$ molecule cm^{-3}) and increase with temperature in this regime (see Figure 1). The bimolecular rate constants for the overall reaction



were obtained in the same manner as for the low temperature reaction, i.e., from the slope of the line fitted through the measured first order decay constants plotted against $[O_2]$, and were fit to an Arrhenius expression

$$k_4 = 6.9 \times 10^{-14} \exp(-2.5 \text{ kcal mol}^{-1}/RT) \text{ cm}^3 \text{ molecule}^{-1} \text{ s}^{-1}$$

In the high temperature region the bimolecular rate constant increases with temperature and has no systematic density dependence. These observations indicate the importance of an irreversible $C_4H_5 + O_2$ reaction path at elevated temperatures which proceeds over an energy barrier.

$C_4H_5 + C_2H_2$ Reaction An attempt was made to observe a possible reaction of C_4H_5 with acetylene at 950K, a reaction indicated as potentially important in the formation of aromatic compounds.¹ There was no increase in the C_4H_5 decay rate over the heterogeneous loss rate when 3×10^{15} molecule cm^{-3} of acetylene was added to the system at a density of 1.2×10^{17} molecule cm^{-3} . Since an increase of a factor of two over the heterogeneous loss could have been observed with C_2H_2 present, an upper limit for the rate constant of the $C_4H_5 + C_2H_2$ reaction at 950K could be established. It is 2×10^{-14} $cm^3 \text{ molecule}^{-1} \text{ s}^{-1}$.

DISCUSSION

The simplest mechanism for the $C_4H_5 + O_2$ reaction which can account for the observations of this study and which is consistent with our current knowledge of the mechanisms of other unsaturated free radicals with molecular oxygen is one which involves the reversible addition of O_2 to the butadienyl radical and a second, irreversible decomposition path for the $C_4H_5O_2$ adduct.

Above 500K, C_4H_5 and O_2 establish and maintain equilibrium while the second, slower, irreversible decomposition reaction of $C_4H_5O_2$ takes place. These reaction pathways account for the observed high-temperature behavior of the $C_4H_5 + O_2$ reaction, including the exponential decay of C_4H_5 when O_2 is in excess, the proportionality of the C_4H_5 decay constants with $[O_2]$, and the lack of density dependence of the overall rate constant for the loss of C_4H_5 . Under these conditions there is a relationship between the phenomenological rate constant k_4 and those of the elementary reactions responsible for the loss of C_4H_5 , $k_4 = K_1 k_3^2 / 2$ (k_3^∞ is the high pressure limit unimolecular rate constant for reaction 3). Using the measured values of K_1 and k_4 an Arrhenius expression for k_3^∞ was determined, $k_3^\infty = 3 \times 10^{12} \exp(-21 \text{ kcal mol}^{-1}/RT) \text{ s}^{-1}$.

The rate constant derived for the decomposition of the adduct is very similar to that obtained for the decomposition of the $C_3H_3O_2$ adduct formed in the reaction of the propargyl radical with molecular oxygen.³ Likewise, the R-O₂ bond strength when R is C_4H_5 is nearly identical with that when R is either C_3H_3 or C_3H_5 (see Table II). The mechanism proposed here for the $C_4H_5 + O_2$

reaction, i.e., reversible addition with a second, irreversible decomposition pathway for the RO_2 adduct, appears common to all $\text{R} + \text{O}_2$ reactions. The initial R-O_2 adducts are formed at rates expected for a simple combination process along an attractive potential. However, the R-O_2 bonds formed by the more stable unsaturated radicals are weaker ($18 - 19 \text{ kcal mol}^{-1}$) than those formed between alkyl radicals and O_2 ($32 - 38 \text{ kcal mol}^{-1}$). The overall reaction pathways observed and the nature of the final products are determined by the relative heights of the barriers to dissociation of the RO_2 adducts back to reactants and to rearrangement of the RO_2 adducts followed by dissociation into oxygenated products. If, as in the case of the allyl radical, the barrier to rearrangement is much greater than that to redissociation, no oxygenated products are observed and the $\text{R} + \text{O}_2$ reaction appears to "turn off" at high temperatures where the equilibrium favors the reactants. If, on the other hand, the barrier to rearrangement is only slightly higher than that to redissociation, the R/RO_2 equilibrium again favors reactants but small amounts of oxygenated products will be observed to be formed as the temperature increases. Such is the case in the C_3H_3 and C_4H_5 reactions. Finally, if the barrier to rearrangement is much less than to redissociation, the $\text{R} + \text{O}_2$ reaction appears to proceed directly to the oxygenated products as in the case of the $i\text{-C}_4\text{H}_7$ reaction.⁴

In conclusion, even at combustion temperatures, reactions of C_3H_3 , C_3H_5 , or C_4H_5 with molecular oxygen are not rapid. They do not effectively remove these intermediates from the pool of radicals. The loss mechanisms for these unsaturated radicals under combustion conditions must also include reactions with themselves to produce larger, unsaturated molecules, reactions with other free radicals (such as O and OH) and perhaps reactions with unsaturated molecules (such as acetylene or butadiene), reactions which could ultimately lead to the production of aromatic compounds.

ACKNOWLEDGEMENT

This research was supported by the Division of Chemical Sciences, Office of Basic Energy Sciences, Office of Energy Research, U.S. Department of Energy under grant No. DE/FG05-89ER14015.

REFERENCES

1. Westmoreland, P. R.; Dean, A. M.; Howard, J. B.; Longwell, J. P. *J. Phys. Chem.* **1989**, *93*, 8171 and references therein.
2. Slagle, I. R.; Ratajczak, E.; Heaven, M. C.; Gutman, D.; Wagner, A. F. *J. Am. Chem. Soc.* **1985**, *107*, 1838.
3. Slagle, I. R.; Gutman, D. *Twenty-First Symposium (International) on Combustion*; The Combustion Institute: Pittsburgh, PA, 1986; p 875.
4. Slagle, I. R.; Bernhardt, J. R.; Gutman, D. *Twenty-Second Symposium (International) on Combustion*; The Combustion Institute: Pittsburgh, PA, 1988; p 953.

Table I: Conditions and Results of the Study of the $C_4H_5 + O_2$ Reaction

a) Experiments to Measure $C_4H_5 + O_2$ Rate Constants

T^a , K	$10^{-16}[M]^b$, molec. cm^{-3}	$10^{-11}[C_3H_8]_0$, molec. cm^{-3}	$10^{-10}[C_4H_5]_0^c$, molec. cm^{-3}	$10^{-14}[O_2]$ Range, molec. cm^{-3}	k_2 , s^{-1}	$10^{14}k_1^d$, $cm^3 \text{ molec}^{-1} s^{-1}$
Room Temperature Reaction						
296	6.00	7.11	3.20	1.93-13.4	37.8	23.
295	12.0	7.22	2.16	1.13-13.7	36.4	32.
299 ^e	12.0	56.6	2.83	1.46-12.5	15.1	31.
296	18.0	2.69	2.64	1.10-9.52	35.9	38.
296	18.0	5.73	2.82	1.77-12.3	34.0	36.
299	18.0	1.27	1.16	1.22-9.34	31.5	38.
High Temperature Reaction						
600 ^e	6.02	7.82	3.46	60.7-216.	26.2	0.72
600 ^e	12.0	28.5	11.0	17.7-172.	27.8	0.94
750 ^e	6.02	50.1	8.94	29.7-188.	18.3	1.2
750 ^e	12.0	20.0	9.00	60.7-215.	29.3	1.1
900 ^e	6.07	18.0	7.65	12.8-256.	26.7	1.8
900 ^e	12.1	6.55	11.1	54.7-237.	26.6	1.6

b) Experiments to Measure the Equilibrium Constant for the $C_4H_5 + O_2$ Reaction^f

T^a , K	$10^{-11}[C_3H_8]_0$, molec. cm^{-3}	$10^5 P_{O_2}$, atm^{-1}	k_2 , s^{-1}	R_{12}	m_1 , s^{-1}	m_2 , s^{-1}	$10^{-3}K_{eq}^g$, atm^{-1}
369	7.81	5.54	23.5	1.58	309.	34.0	32.2
369	7.82	9.37	19.0	2.70	318.	29.9	31.9
374	6.78	7.73	27.0	1.97	345.	33.2	27.0
374	6.78	6.62	22.4	1.47	333.	34.9	25.4
379	7.85	10.1	21.7	1.47	374.	38.9	17.2
379	11.7	23.7	23.1	3.86	674.	41.9	17.5
384	14.5	25.2	29.9	2.63	679.	45.0	11.1
384	15.4	44.3	28.4	4.37	833.	43.8	10.3
389	7.95	26.2	31.0	3.15	847.	54.7	13.0
389	14.9	26.2	31.4	2.64	702.	41.1	10.5
389	14.7	45.7	34.2	4.86	1193.	52.5	11.0
394 ^e	107.	46.0	22.8	2.43	1215.	57.5	5.74
394	13.6	53.4	21.3	3.27	1071.	54.0	6.65
399	9.96	30.5	30.8	1.65	674.	53.4	6.06
399	9.84	56.6	26.3	2.26	892.	53.0	4.37

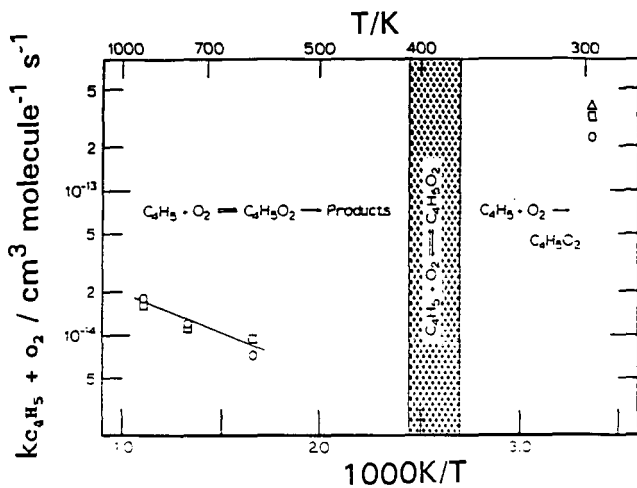


Figure 1. Arrhenius plot of measured second-order rate constants for the $C_4H_5 + O_2$ reaction. Shaded area indicates the temperature region where equilibrium was the dominant process observed. \circ indicates experiments conducted at a density of 6×10^{16} , \square at 1.2×10^{17} , and Δ at 1.8×10^{17} molecule cm^{-3} .

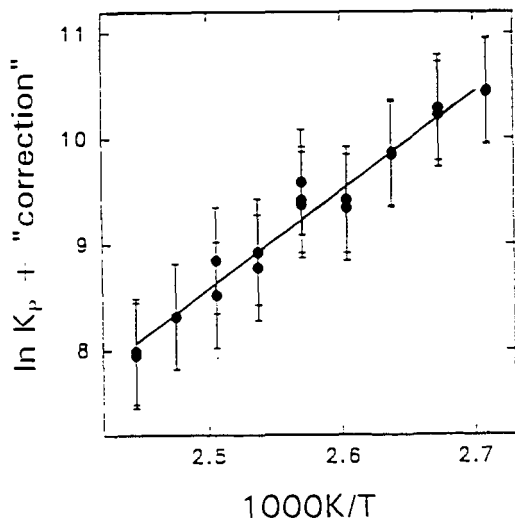


Figure 2. Modified van't Hoff plot of measured equilibrium constants for the $C_4H_5 + O_2$ reaction.

Table I (continued)

T ^a , K	10 ⁻¹¹ [C ₃ H ₃] ₀ , molec. cm ⁻³	10 ⁵ P _{O₂} , atm ⁻¹	k ₂ , s ⁻¹	R ₁₂	m ₁ , s ⁻¹	m ₂ , s ⁻¹	10 ⁻³ K _{eq} ^b , atm ⁻¹
404	20.2	45.6	37.8	1.39	921.	76.3	3.54
409	20.2	46.2	29.4	0.809	580.	69.3	2.42
409	12.6	57.9	29.8	1.23	1001.	74.5	2.51

^aTemperature variations: 350-450±3K, 600±2K, 750±4K, 900±5K

^bM = He + O₂

^cUpper limit to [C₄H₅]₀ estimated assuming that one half of the precursor that decomposes produces C₄H₅.

^dEstimated error limits are ±20% for room-temperature rate constants and ±30% for high temperature rate constants.

^e248 nm photolysis light used in this experiment; 193 nm used in all other experiments.

^fC₄H₅ ion signal, I(t), fit to expression I(t) = Aexp(-m₁t) + Bexp(-m₂t). [M] = 1.2×10¹⁷ molecule cm⁻³

^gK_p = (R₁₂/P_{O₂}){1 + [(R₁₂ + 1)(m₂ - k_w)]/[R₁₂(m₁ - m₂)]}²; R₁₂ = A/B; estimated error limits: ±50%.

Table II: Comparison of Thermodynamic Variables for R + O₂ Reactions Involving Unsaturated Free Radicals

R	ΔH ^o ₂₉₈ , kcal mol ⁻¹	ΔS ^o ₂₉₈ , cal mol ⁻¹ K ⁻¹	Ref.
C ₃ H ₃	-18.9±1.4	-31.3±2.9	3
C ₃ H ₅	-18.2±0.5	-29.2±1.2	2
C ₄ H ₅	-18.7±0.8	-29.2±2.2	Current Study